



# ORGANOCLAY PLURONIC F68 – MONTMORILLONITE, AS A SUSTAINED RELEASE DRUG DELIVERY VEHICLE FOR PROPRANOLOL HYDROCHLORIDE

Seema<sup>[a]</sup> and Monika Datta<sup>[a]\*</sup>

**Keywords:** Montmorillonite; Pluronic F68; organoclay; propranolol hydrochloride; adsorption; sustained release drug delivery.

Short half life of propranolol hydrochloride (PPN), an antihypertensive drug is a prime requirement to develop a formulation which could sustain the release of PPN in the human body and also eliminate daily multiple dosage of propranolol. In this study organoclay Pluronic F68 modified montmorillonite (Mt) has been explored as a sustained release carrier for oral delivery of PPN. The developed organoclay PF68-Mt was compared for adsorption capacity of PPN with pristine Mt. A detailed and systematic study to evaluate the effect of pH, time and initial PPN concentration on drug loading capacity of organoclay PF68-Mt and pristine Mt has been evaluated. The synthesized PF68-Mt-PPN composites were characterized by XRD, FTIR, TGA techniques. XRD studies suggested the intercalation of PPN within the pristine Mt and organoclay PF68 - Mt. In vitro drug release profile of PPN from organoclay PF68-Mt composites is compared with that of pristine Mt and the pure PPN, in simulated gastric and intestinal fluids. The release profile of loaded PPN in organoclay PF68-Mt shows pH dependent release in simulated gastrointestinal fluid. The release behaviour of PPN from PF68-Mt-PPN composites was appeared to be in more sustained manner than pristine Mt and pure PPN over a period of 24 hours. This study suggests that the modification of Mt with a non ionic tri block co polymer Pluronic F68 provides better controlled on the release of PPN as compared to pristine Mt and pure drug. The obtained PF68-Mt-PPN composites with high drug loading capacity and sustained drug release characteristics supposed to be a better oral drug delivery system, for a highly hydrophilic low molecular weight antihypertensive drug PPN. The PF68-Mt-PPN composites developed have the potential to minimize the drug dosing frequency and hence improving the patient compliance. Thus, proposing a new promising formulation for oral sustained release drug delivery.

\*Corresponding Author

Fax: +91-01127666605

E-Mail: [monikadatta\\_chem@yahoo.co.in](mailto:monikadatta_chem@yahoo.co.in)

[a] Analytical Research Laboratory, Department of Chemistry, University of Delhi, Delhi-110 007, India

mechanisms of the reactions that the clay minerals can have with the organic compounds.<sup>3</sup> Depending on the layer charge of the clay mineral and the chain length of the organic ion, different arrangements of organic molecules between the layers can be formed.

## INTRODUCTION

Recently there is a growing use of clays in delivery technology in order to confer slow release properties of the active ingredient, which is of particular interest in pharmaceutical industry.<sup>1,2</sup>

Organoclays are extensively used in a wide range of applications as a basis for the synthesis of clay polymer nanocomposites, for photophysical applications, paints, cosmetics, refractory varnish, thixotropic fluids, or geochemical barriers in waste landfills.<sup>3-7</sup> Surface modifications of clay minerals in the form of organoclays allows the creation of new materials and new applications. However these materials are not widely explored in the area of drug delivery.

Organoclays combine the properties of natural clays such as a high surface area and a hydrophobic surface which allow the adsorption of organic compounds or the dispersion of clays into polymers.<sup>3,6,8</sup> Another feature is the strong increase of the interlayer height, comparatively small for the clay before modification, which makes easier the insertion of guest molecules whose orientations follow those of the previously adsorbed molecules used for the manufacture of organoclays.<sup>9,10</sup> The synthesis of organoclays is based on the

Being non toxic, biocompatible and FDA approved, montmorillonite (Mt) a smectite clay mineral is extensively explored for oral drug delivery applications in recent years. The advantageous characteristic physicochemical properties of Mt provides it all the properties of an ideal drug delivery vehicle.<sup>1,2,11-14</sup>

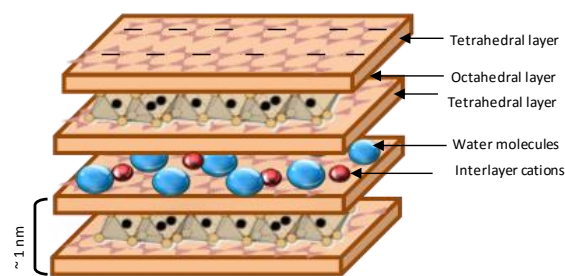


**Figure 1.** Structure of montmorillonite

Organo-montmorillonites, are mainly obtained by intercalating cationic surfactants such as quaternary ammonium compounds into the interlayer space through ion exchange.<sup>3,15-16</sup> The interlayer spacing of these organoclays generally increases as the surfactant loading increases and reaches a saturation limit which corresponds to or is larger than the clay cation exchange capacity (CEC).<sup>11,15-16</sup> However, the intercalation of a long alkyl tail surfactant

within the interlayer space is irreversible and prevents any further cationic exchanges which limit, as a result, the potential applications of the nanocomposites and/or the innovation of new hybrid materials.<sup>17,18</sup> Therefore, the synthesis of organoclays by using other surfactants is a new area of interest.

Pluronic F-68 a triblock copolymer has been approved for biomedical applications by US food and drug administration.<sup>19</sup> The properties of amphiphilic poly(ethylene oxide)- $\beta$ -poly-(propylene oxide)- $\beta$ -poly(ethylene oxide) (PEO-PPO-PEO) block copolymers in aqueous media have attracted a great deal of interest because of several important aspects.<sup>19-20</sup> PEO-PPO-PEO copolymers are commercially available surfactants (pluronics, synperonics, poloxamers), whose molecular weight and PEO/PPO composition ratio vary within a wide range. In water above their critical micelle concentration (CMC) value they usually spontaneously form nanosized core-shell micelles having a hydrophobic core composed predominantly of PPO segments and a shell dominated by hydrated PEO segments.<sup>21-22</sup> The PEO blocks have available functionality to which receptor-specific ligands could be attached. That is why the PEO-PPO-PEO copolymers meet the specific requirements for various applications, such as dispersion stabilization, emulsification, detergency, foaming, lubrication etc.<sup>19-22</sup> presently the PEO-PPO-PEO copolymers are being intensively evaluated as potential drug and gene delivery systems for multiple pharmaceutical applications as well as for diagnostic imaging as carriers for various contrasting agents. The hydrophobic PPO core may serve as a container for water insoluble drugs while the hydrophilic PEO shell provides steric stability.<sup>19</sup>

Propranolol hydrochloride, [(2RS)-1-(1-methylethyl)-amino-3-(naphthalen-1-yloxy)propan-2-ol hydrochloride] is widely used for the treatment of hypertension. The dose of propranolol hydrochloride (PPN) ranges from 40 to 80 mg day<sup>-1</sup>.<sup>23</sup> Due to shorter half life (3.9 hours) the conventional PPN tablets has to be administered 2 or 3 times daily so as to maintain adequate plasma levels of drug.<sup>24</sup> Multiple drug administration results either in manifestation of side effects or reduction in drug concentration at the receptor site. Thus, the development of sustained-release dosage forms would clearly be advantageous.<sup>4</sup> Some researchers have formulated oral sustained-release products of PPN by various techniques.<sup>12, 25-27</sup>

In the present study FDA approved 2:1 smectite clay mineral Mt and a non ionic surfactant Pluronic F68 has been selected because of their structural, biological and industrial importance for the synthesis of organoclay PF68-Mt. To the best of our knowledge this system is reported for the first time and being further explored as a sustained release drug delivery vehicle for Propranolol hydrochloride (PPN) as a model drug.

The synthesized organoclay PF68-Mt was characterized by several complementary techniques including X-Ray diffraction (XRD), Fourier transform infrared spectroscopy (FTIR), TGA, DSC, and SEM.

A systematic study was carried out to obtain PPN loaded organoclay PF68-Mt composites by optimizing various experimental conditions for maximum adsorption capacity as a sustained release drug delivery vehicle. The obtained PF68-Mt-PPN composites were compared for their physicochemical properties and in vitro drug release profile with pristine Mt-PPN composites developed under similar conditions.

The obtained preliminary results suggest the potential of the synthesized organoclay PF68-Mt-PPN composites for oral and sustained release drug delivery of PPN for the treatment of hypertension around the clock.

## EXPERIMENTAL

### Materials

Montmorillonite KSF, PPN (purity >99 %) and Pluronic F-68 with a molecular weight equal to 8500 Dalton were obtained from Sigma Aldrich St. Louis USA. Analytical grade HCl, KCl, NaOH, Potassium dihydrogen phosphate was ordered by MERCK (Germany). All other reagents whether specified or not were of analytical grade. Water used in the experiments was deionized and filtered (Milli-Q Academic, Millipore, France).

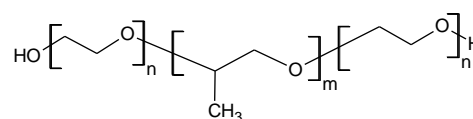


**Figure 2.** Structure of Pluronic F68,  $n = 75$  oxyethylene units,  $m = 30$  oxypropylene units

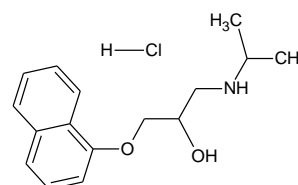


**Figure 3.** Structure of propranolol.HCl

### Synthesis of organoclay Pluronic F68-montmorillonite

A nonionic triblock copolymer PF68 was selected as surfactant for the synthesis of organoclay PF68-Mt. In brief an aqueous Mt dispersion (1% w/v) was allowed to swell overnight at constant magnetic stirring of 500 rpm to form a stable Mt dispersion. A 2 % (w/v) PF68 solution was prepared separately and added gradually to the Mt dispersion to form a reaction media (above CMC of PF68) within a period of 2 hours followed by 6 hours stirring at normal room temperature. The resulted hydrophobic reaction media was centrifuged at 20,000 rpm followed by several washings to remove the unreacted PF68.

The obtained residue was lyophilized at  $-45\text{ }^{\circ}\text{C}$  and pressure of 30 mTorr. Thus obtained organoclay PF68-Mt was characterized with suitable analytical techniques as discussed under characterization section and further used as an adsorbent for the PPN.

#### pH Stability study of the aqueous PPN Solution

To start with the experiment, stability of PPN molecule as a function of pH was evaluated in the pH range of 1-12. The pH of the 10 ppm drug solutions was maintained using 0.1N HCl and NaOH solutions using pH meter (Eutech instruments). The solutions thus prepared were analysed spectrometrically at  $\lambda_{\text{max}}$  of 289 nm.

#### Synthesis of organoclay Mt-PF68-PPN composites and pristine Mt-PPN composites

In order to investigate the interaction of PPN with organoclay PF68-Mt, PF68-Mt-PPN composites were synthesized as per the reported method with certain modification as function of time, pH, Mt content and PPN content.<sup>14</sup>

Effect of pH on the adsorption efficiency of PPN on PF68-Mt, was investigated by treating 50 ml of 200 ppm aqueous PPN solution with organoclay PF68-Mt (0.1 g) in the pH range of 1 to 11 and allowed to stir on a magnetic stirrer for a period of 2 hours at 1000 rpm. In the next step, effect of contact time on the adsorption efficiency of PPN onto PF68-Mt surface was evaluated. The 50 ml aqueous PPN solution of 200 ppm concentration at pH 9.6 was treated with organoclay PF68-Mt (0.1 g) over a period of 0.25, 0.5, 0.75, 1, 2 and 3 h on a magnetic stirrer at 1000 rpm. Further, the effect of initial drug concentration on the adsorption capacity of PPN on PF68-Mt was evaluated. The 0.1 g of PF68-Mt was treated with 50 ml of PPN solution in the concentration range of 2 mg-20 mg/50 ml (40-400 mg  $\text{L}^{-1}$ ) at the original aqueous drug solution pH (9.6) and allowed to stir on a magnetic stirrer for a period of 2 h at 1000 rpm.

After desired reaction time, PF68-Mt-PPN dispersion were centrifuged with 20,000 rpm for 30 minutes at  $10\text{ }^{\circ}\text{C}$  (Sigma, Sartorius, 3K30). The free PPN concentration in the supernatant were determined using UV-visible spectrophotometer (Analytic Jena) at 289 nm from the Lambert-Beer's plot and the percentage of the drug adsorbed, being calculated using equation 1.

$$\text{Drug adsorbed (\%)} = \frac{C_i - C_e}{C_i} \times 100 \quad (1)$$

where

$C_i$  is the initial drug concentration ( $\text{mg L}^{-1}$ ) and

$C_e$  is the concentration of the drug ( $\text{mg L}^{-1}$ ) in the supernatant at the equilibrium stage.

The amount of drug adsorbed  $q_e$  ( $\text{mg g}^{-1}$ ); was calculated via the mass-balance relationship as per the equation 2.

$$q_e = \frac{(c_i - c_e)V}{m} \quad (2)$$

where

$V$  is the volume of the reaction media in litre and

$m$  is the mass of organo-Mt used for the studies in grams.

In order to compare and evaluate the effect of pristine Mt, experiments were also performed to synthesized pristine Mt-PPN composites and evaluated for drug adsorption capacity in a same manner as a function of time, pH, and PPN content as discussed above.

#### Characterizations of organoclay PF68-Mt, pristine PPN-Mt composites and PF68-Mt-PPN composites

Powder X-ray diffraction (PXRD) measurements of pristine Mt, organoclay PF68-Mt, PF68-Mt-PPN and pristine Mt-PPN composites were performed on a powder X-ray diffractometer (XPRT PRO Pananalytical, model PW3040160, Netherland) the measurement conditions were Cu K  $\alpha$  radiation generated at 40 kV and 30 mA as X-ray source  $2-40^{\circ}$  ( $2\theta$ ) and step angle  $0.01^{\circ} \text{ s}^{-1}$ . FTIR spectra of the same samples were recorded with an FTIR spectrophotometer (Perkin Elmer, Spectrum BXTIR Spectrometer) using the KBr (Merck, Germany) disc method. Thermogravimetric analysis was carried out within  $30 - 700\text{ }^{\circ}\text{C}$  at  $10\text{ }^{\circ}\text{C min}^{-1}$  in nitrogen flow (TGA 2050 Thermal gravimetric Analyzer. Differential scanning calorimetric studies were conducted on DSC instrument (DSC Q200 V23.10 Build 79). The samples were purged with dry nitrogen at a flow rate of  $10\text{ ml min}^{-1}$  and the temperature was raised at  $5\text{ }^{\circ}\text{C min}^{-1}$ . For surface morphology analysis, one drop of the samples was mounted on a stubs; sputter coated with gold in a vacuum evaporator and photographed using a scanning electron microscope model (ZEISS EVO 40) with an accelerating voltage of 20 KV. For particle shape and size, samples were examined by mounting a sample drop on the carbon coated copper grids, dried overnight and photographed using a transmission electron microscope (TECNAI G2 T30, U-TWIN) with an accelerating voltage of 300 kV. Zeta potential of the 0.01 % aqueous suspension of the samples were determined using Malvern zeta sizer Nano ZS.

#### In vitro drug release studies

In vitro drug release studies of pristine Mt-PPN composites and organoclay PF68-Mt-PPN composites, were evaluated in two dissolution media consisting of simulated intestinal fluid (PBS, pH 7.4) and simulated gastric fluid (HCl, pH 1.2) using the dialysis bag technique.<sup>28</sup> Both the dissolution media were prepared as per the reported method.<sup>29</sup>

Dialysis membranes (Sigma-Aldrich, Mw. 8405) were equilibrated overnight with the dissolution medium prior to experiments.

Weighed amount of pristine Mt-PPN composites and organoclay PF68-Mt-PPN composite with known drug content were taken in 5ml of dissolution media in the dialysis bag. Enclosed dialysis bag was dipped into the receptor compartment containing 100 ml dissolution medium, which was closed and maintained with 100 rpm at  $37 \pm 0.5$  °C. 5 ml of aliquote was withdrawn at regular time intervals and the same volume was replaced with a fresh dissolution medium maintained at 37°C. The withdrawn aliquotes were analyzed for PPN content by UV-Visible spectrophotometer (Analytic Jena) at 289 nm. Cumulative percentage of drug release was calculated by Lambert-Beer's plot of PPN obtained in the same dissolution media.

## RESULTS AND DISCUSSION

### Characterization of Organoclay PF68-Mt

#### XRD studies

Pristine Mt showed a characteristic diffraction peak at  $2\theta$  of  $6.4^\circ$  (001 plane) representing  $d$  spacing of 13.4 Å.<sup>30</sup> In case of synthesized organoclay PF68-Mt a shifting in  $2\theta$  value from  $6.4^\circ$  to  $4.6^\circ$  and stronger intensity was observed (Figure 4). According to Bragg's law, shifting in  $2\theta$  value from higher diffraction angle to lower diffraction angle is because of increase in  $d$  spacing and intercalation of an organic moiety.<sup>30,31</sup> An increase of 9.2 Å was observed on intercalation of PF68 in Mt layers corresponding to the increase in  $d$  spacing from 13.6 Å to 18.8 Å.

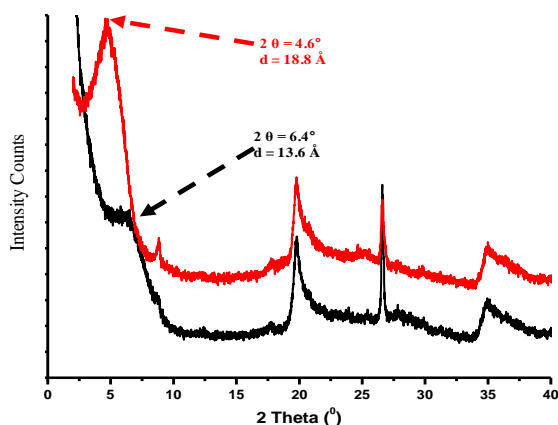


**Figure 4.** XRD pattern of Pristine Mt, organoclay PF68-Mt

Pluronic F68 a non ionic triblock copolymer of poly oxy ethylene, poly oxy propylene as already discussed earlier is known to form micelles in aqueous media above its critical micelle concentration (CMC).<sup>19,22</sup> During the synthesis process of organoclay PF68-Mt, these PF68 micelles supposed to interact with the interlayer water molecules and polar groups of Mt, resulting in intercalation of PF68 with increase in  $d$  spacing from 13.6 to 18.8 Å.

A schematic representation for synthesis of organoclay PF68-Mt with PF68 is represented in Figure 5.

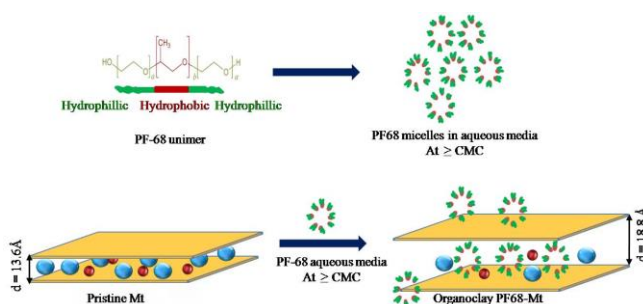


**Figure 5.** Schematic representation for the synthesis of organoclay PF68-Mt

#### FTIR studies

In order to confirm the presence of surfactant PF68 within the interlayer region of the Mt, FT-IR spectra were recorded in the region 400-4000  $\text{cm}^{-1}$ . In the IR spectrum of Mt, the band at 1049  $\text{cm}^{-1}$  has been assigned to Si-O stretching and is the characteristic band of Mt. The band at 3428  $\text{cm}^{-1}$  and 3629  $\text{cm}^{-1}$  has been assigned to H-O-H stretching vibrations from interlayer water and O-H stretching vibrations of the structural OH group. The absorption band at 1639  $\text{cm}^{-1}$  corresponds to H-O-H bending. The absorption bands at 538  $\text{cm}^{-1}$  and 474  $\text{cm}^{-1}$  are strong bending vibrations corresponding to Al-O-Si and Si-O-Si respectively.<sup>32-34</sup> (Figure 6).

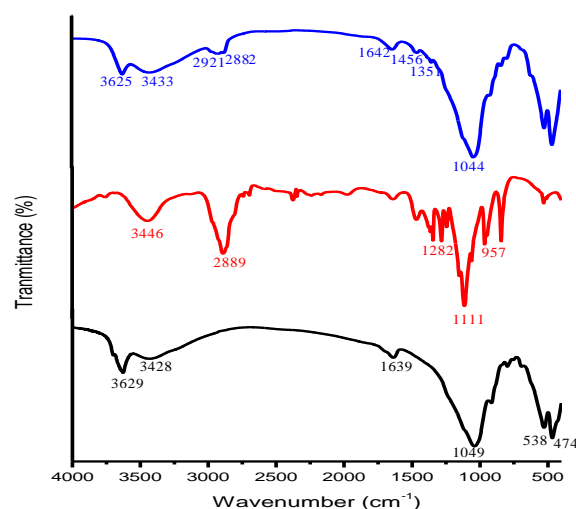


**Figure 6.** FTIR spectra of pristine Mt, Pluronic F68, organoclay PF68 - Mt

The major peaks observed around 3446  $\text{cm}^{-1}$  in PF68 is assigned to the vibrations of hydroxyl (-OH) groups.<sup>35</sup> A strong absorption band at 2889  $\text{cm}^{-1}$  was observed. The characteristic peaks at 957  $\text{cm}^{-1}$  and 1111  $\text{cm}^{-1}$  in PF68 were due to C-O symmetrical structure and C-O asymmetrical stretching vibrations of ether groups.

The peak at  $1282\text{ cm}^{-1}$  is assigned to  $-\text{CH}_2$  group vibration of PF68.<sup>35</sup> The presence of functional groups of PF68 on the surface of Mt is verified by peaks at about  $2921\text{ cm}^{-1}$  and  $2882\text{ cm}^{-1}$  characteristic of the aliphatic C–H antisymmetric and symmetric vibrations respectively from the methylene group of PF68. Beside two new bands at  $1351\text{ cm}^{-1}$  and  $1456\text{ cm}^{-1}$  were also appeared. The presence of these bands in organoclay PF68-Mt indicates that PF-68, the neutral surfactant could interact with the Mt layers through an ion-dipole type interaction or hydrogen bonding between the hydrophilic or polar part of the PF68 and the water molecules around the exchange cations of the Mt.<sup>36,37</sup>

#### TG-DTA studies

The pristine Mt shows high thermal stability with weight loss of 10 % from 30-140 °C and is attributed to the loss of adsorbed and interlayer water followed by dehydroxylation in the temperature range from 600-750 °C respectively.<sup>12</sup> In case of organoclay PF68 a weight loss of 3.5 % was observed because of the loss of surface sorbed water in the temperature range of 25-35 °C (Figure 7).

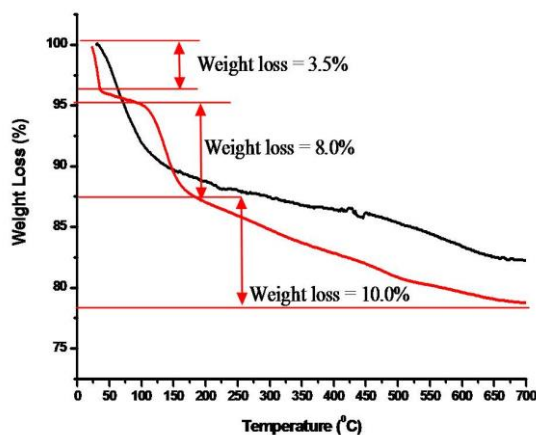


Figure 7. TG pattern: pristine Mt, organoclay PF68 - Mt

A second step weight loss of 8 % was observed from 105 °C to 180 °C due to the replacement of interlayer water by organic PF68 which thermally unstable in this region. In third step from 180 °C to 700 °C, a final weight loss of 10 % was observed and combinedly attributed to the thermal decomposition of the PF68 and structural hydroxyl groups.

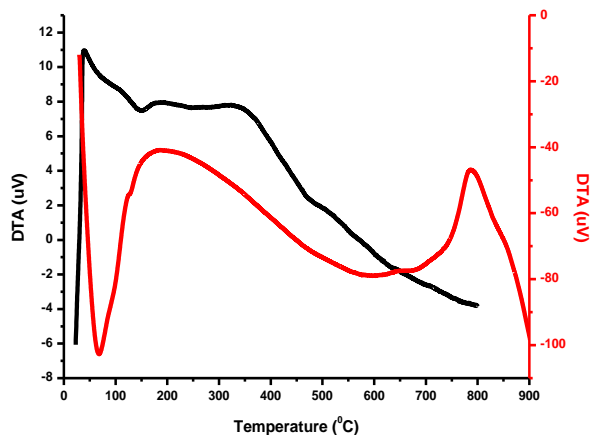


Figure 8. DTA pattern pristine Mt, organoclay PF68-Mt

The DTA thermo gram of pristine Mt resulted in a strong endothermic peak at 80 °C and broad endothermic peak at 600 °C corresponding to evaporation of the adsorbed water and loss of structural water respectively.<sup>38,39</sup> However, in case of organoclay PF-68 DTA pattern (Figure 8), an endothermic event at 149 °C corresponding to decomposition of intercalated surfactant moiety was observed.<sup>36,37</sup> This event is followed by an exothermic pattern which might be attributed to the thermal degradation of intercalated PF68 moiety.

#### DSC studies

In pristine Mt, the broad endotherm centered at 110 °C is attributed to the dehydration of adsorbed water (Figure 9). In case of organoclay PF68-Mt a sharp endotherm at 63.9 °C corresponds to melting of intercalated PF68 within Mt layers was observed. Second endotherm at 153 °C is attributed to the decomposition of organic copolymer species<sup>37,38</sup> followed by broad endothermic region in the range of 285-355 °C attributed to the thermal degradation of PF68 within Mt layers.

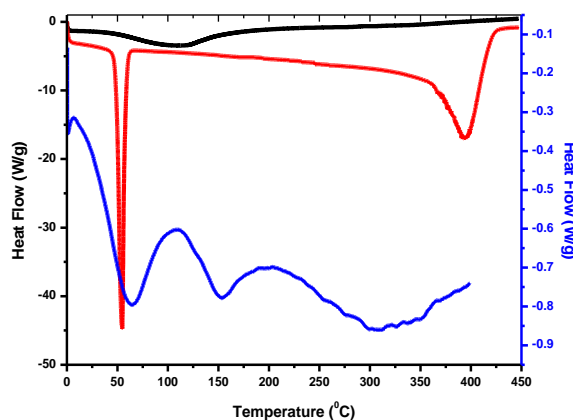


Figure 9. DSC curves: pristine Mt, Pluronic F68, organoclay PF68 - Mt

#### Surface morphology studies

Scanning electron microscopic (SEM) studies indicates that surface morphology of organoclay PF68-Mt was relatively porous compared to the pristine Mt. The particle size of PF68 modified Mt was found in the range of 1 to 2  $\mu\text{m}$  (Figure 10) by SEM analysis.

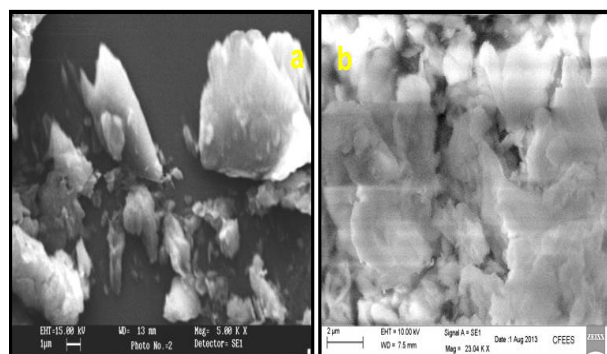
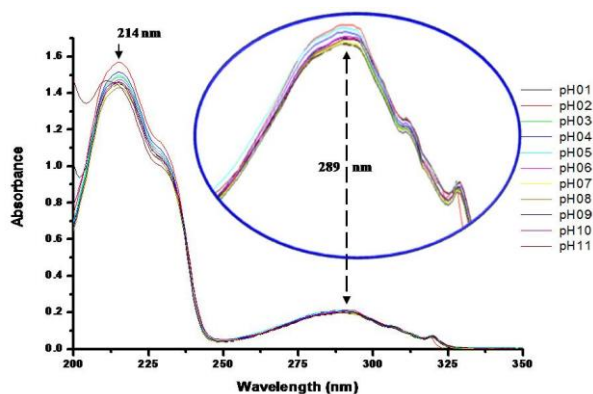


Figure 10. SEM of Mt (a) and PF68 modified Mt (b)

### pH Stability study of the aqueous PPN solution

The pH stability of the aqueous PPN solution in the pH range 1 to 11 was investigated spectrophotometrically. The UV absorption spectra of PPN show two absorption peaks at 214 nm and 289 nm corresponding to different electronic transitions of the molecule. It has been found that PPN maintains its stability (Figure 11) within the experimental pH range as there is no change in the absorption spectra of PPN molecule was observed.



**Figure 11.** Absorption spectra of PPN as a function of pH of the PPN aqueous solution

### Effect of pH on adsorption efficiency

The pH of the drug solution has always played a crucial role in adsorption process. pH effect of PPN aqueous solution on pristine Mt and organoclay PF68-Mt surface is shown in Figure 12. The results suggest that in the pH range of 5-10 adsorption of PPN on pristine Mt surface remain almost constant. But there was sharp decrease in adsorption when the pH was above 10 and below 5 up to 3. Whereas in case of organoclay PF68-Mt, the adsorption of PPN on PF68-Mt was found increase from (50 % to 85 % of 200 ppm drug solution) in the pH range of 2-10 followed by decrease up to 61 % at pH 11. This can be explained on the basis of  $pK_a$  value of PPN ( $pK_a = 9.5$ ).<sup>25</sup>

It has been reported that PPN undergo ionization under different pH conditions and about 75.8 % of it is in protonated form at pH 9 which increases to 99.7% and 99.9 % at pH 7 and pH 5 respectively. Hence, the high adsorption of PPN on pristine Mt surface (96-98 %) was observed at 200 ppm attributed to the strong affinity of negatively charge Mt surface for protonated form of PPN. However, decrease in adsorption (%) below pH 5 could be because of the competition between high concentrations of  $H^+$  ions present at low pH which get adsorbed on the Mt surface. Besides at high pH values, the species of negative PPN increases and slightly reduce the adsorption of drug at pH 11 due to repulsion between Mt and drug. With increase in pH, PPN exist in the protonated form and positive charge on the surface of the PF68-Mt decreases resulting in high adsorption of PPN with PF68-Mt layers. At pH above  $pK_a$ , PPN is negatively charged, which restricts the adsorption of PPN as a result of the repulsive force between PPN and the negatively charged surface of the PF68-Mt leading to decreased adsorption % at pH 11.

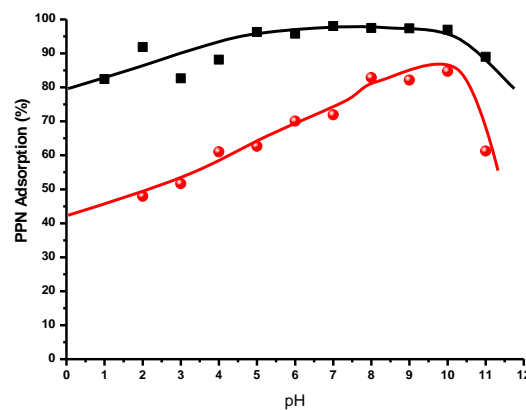


**Figure 12.** Effect of pH of PPN solution on adsorption efficiency at Mt, PF68-Mt with conc. 200 ppm and time 2 h

### Effect of time on adsorption efficiency

Time dependent adsorption of PPN on pristine Mt shows 82 % adsorption of PPN (200 ppm) within a period of 30 minutes (Figure 13). The adsorption (%) increased up to 85 % in 2 hours and tends to decrease up to 84 % in 3 h. Negative surface charge as well as the rapid ion exchange process between Mt interlayer  $Na^+$  ions and cationic PPN molecule is mainly attributed for the higher uptake of PPN. Time dependent adsorption of PPN on PF68-Mt shows 76.8 % adsorption of PPN (200 ppm) within a period of 30 minutes which increased up to 78.3 % over a period of 3 h.

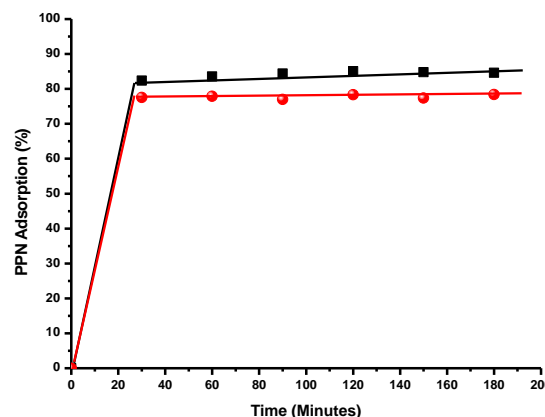


**Figure 13.** Effect of time on adsorption efficiency at pristine Mt, Organoclay PF68-Mt with conc. 200 ppm and pH 9.6

### Effect of PPN concentration on adsorption efficiency

At the natural pH of PPN (pH 9.6), the adsorption of PPN on pristine Mt and organoclay PF68-Mt is affected by its initial amount present in the solution (Figure 14). As the PPN amount in the solution increases from 2 to 4 mg (40 to 80 ppm), the adsorption % increases from 92 % to 95 %. With further increase in the initial drug amount up to 20 mg ( $400 \text{ mg L}^{-1}$ ) the adsorption % decreases upto 49.5 % and 67.6 % whereas the total amount of drug adsorbed increases from 1.8 mg to 9.9 mg and 1.86 mg to 12.8 mg for pristine Mt and organoclay PF68-Mt respectively. Therefore, it could be concluded that due to the higher availability of the adsorption sites, nearly 100 % adsorption was obtained at lower concentration of initial drug.

Modification of Mt with PF68 might have increased the surface area of the Mt, which has provided the larger adsorption site for interaction with PPN resulting in high adsorption % of PPN on organoclay PF68-Mt as compared to pristine Mt. The adsorption capacity  $127 \text{ mg g}^{-1}$  and  $171 \text{ mg g}^{-1}$  was observed for pristine Mt and organoclay PF68-Mt respectively.

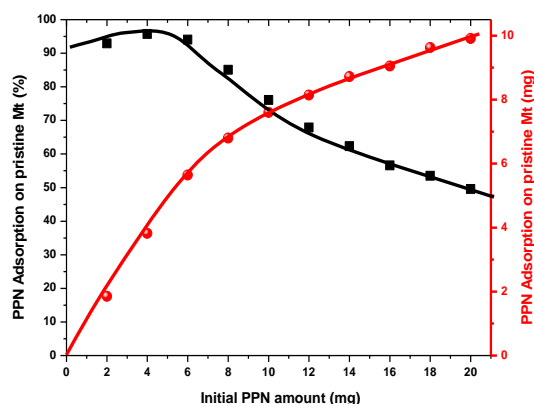


**Figure 14.** Effect of initial amount of PPN solution on adsorption efficiency of pristine Mt with equilibrium time 2 h and pH 9.6

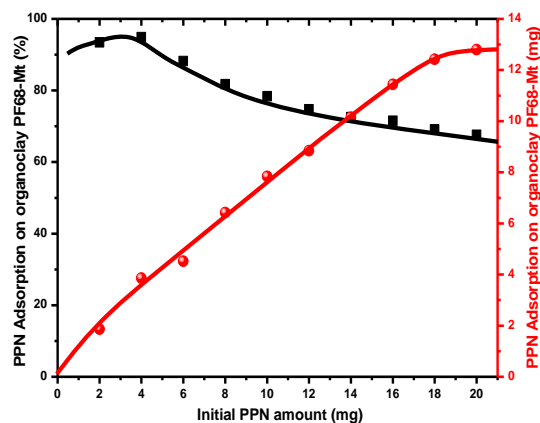


**Figure 15.** Effect of initial concentration of PPN solution on adsorption efficiency of organoclay PF68-Mt with time equilibrium 2 h and pH 9.6

#### Characterization of pristine Mt-PPN composites and organoclay PF68-Mt-PPN composites

##### XRD Studies

The XRD pattern of pristine Mt, pure PPN and pristine Mt-PPN composites are shown in **Figure 16**. Mt showed a distinct diffraction pattern (001 plane) at  $2\theta = 6.4^\circ$  representing a  $13.4 \text{ \AA}$  thickness of the Mt layer.<sup>30</sup> The Mt-PPN composites prepared at optimized conditions did not present the PXRD pattern of drug alone, suggesting that drug was in an amorphous form. In case of Mt-PPN composites a shifting in  $2\theta$  value from  $6.4^\circ$  to  $5.6^\circ$  and stronger intensity was observed. A previous study,<sup>25</sup> suggest stronger intensity of the basal spacing peak occurs when the drug molecule was intercalated within the Mt layers. According to Bragg's law, shifting in  $2\theta$  value from higher diffraction angle to lower diffraction angle is because of increase in  $d$  spacing. This indicates increase in the interlayer spacing upon intercalation of PPN in the Mt layers

from  $13.6 \text{ \AA}$  to  $15.6 \text{ \AA}$  with the replacement of interlayer cation by PPN. Subtracting the Mt layer thickness ( $9.6 \text{ \AA}$ ) from the  $d$  spacing ( $15.6 \text{ \AA}$ ) of the Mt-PPN complex, the Mt layer thickness was estimated to be  $6 \text{ \AA}$ .<sup>30-31</sup>

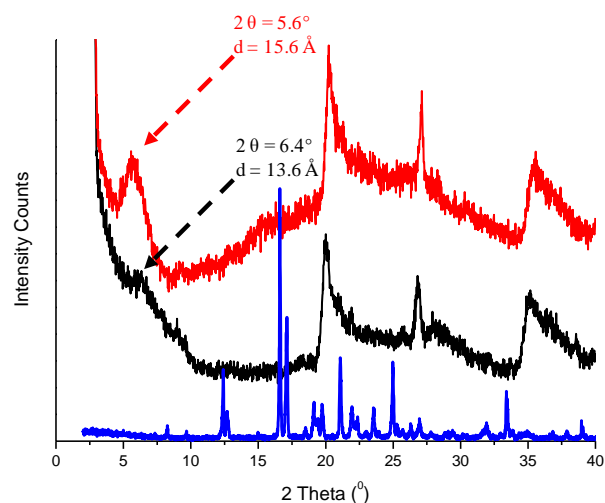


**Figure 16.** XRD pattern of pristine Mt, Mt-PPN composites, pure PPN

The result suggested that intercalated PPN form a monolayer with lying flat on the Mt surface as shown in Figure 17.



**Figure 17.** Diagrammatic representation of PPN intercalation within Mt layers

When organoclay PF68-Mt with  $d$  spacing of  $18.8 \text{ \AA}$  was used as adsorbent for PPN the  $2\theta$  value of optimized sample shift from lower to higher diffraction angle of  $4.6^\circ$  to  $4.9^\circ$  with decrease in  $d$  spacing from  $18.8 \text{ \AA}$  to  $18.05 \text{ \AA}$  (Figure 18).

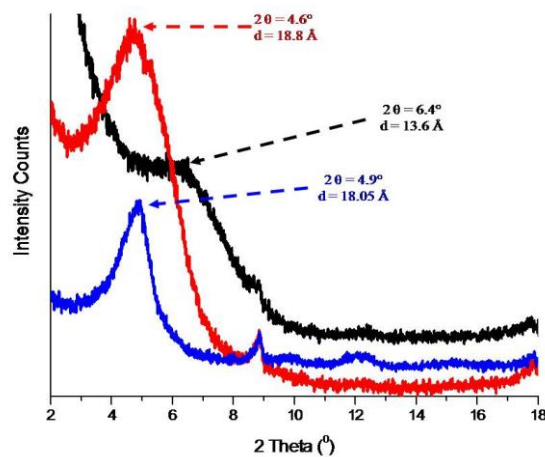


**Figure 18.** XRD pattern of pristine Mt, PF68-Mt, PF68-Mt-PPN complex

The decrease in  $d$  spacing might be attributed to the replacement of certain intercalated PF68 (surfactant) moiety with PPN molecule. In order to accommodate the PPN molecule within the Mt layers, space is created by replacement of certain PF-68 (surfactant) molecule and the interaction of hydrophilic PEO with hydrophilic PPN moiety might be suggested.

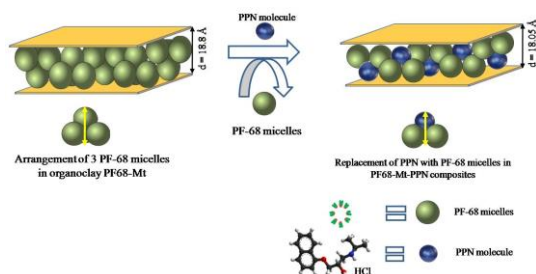
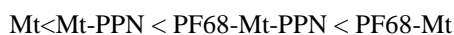


**Figure 19.** Diagrammatic representation for intercalation of PPN within PF68-Mt

It has been well established, that above CMC, PF-68 molecule arranges itself into the spherical micellar form.<sup>19-22</sup> So, it can be suggested that because of hydrophilic-hydrophilic interaction the PPN molecule might get placed within hydrophilic corona of the PF68 micelles, (Figure 19) and hence being smaller in size, no significant change in the  $d$  spacing of PF68-Mt was observed.

On the basis of obtained XRD results it could be concluded that pristine Mt, organoclay PF68-Mt, pristine Mt-PPN composites and organoclay PF68 PF68- Mt-PPN composites followed the order of  $d$  spacing as:



#### FT-IR studies

The FT-IR spectrum of pristine Mt, pure PPN and Mt-PPN composites prepared by adsorption/ion exchange process is shown in Figure 20. The FT-IR spectra of PPN revealed the presence of peaks at 3323 and 3283  $\text{cm}^{-1}$  corresponding to N-H and O-H stretching peaks. The aryl alkyl ether displayed a stretching band at 1268  $\text{cm}^{-1}$  and the peak at 798  $\text{cm}^{-1}$  was due to substituted naphthalene.<sup>24,41-42</sup>

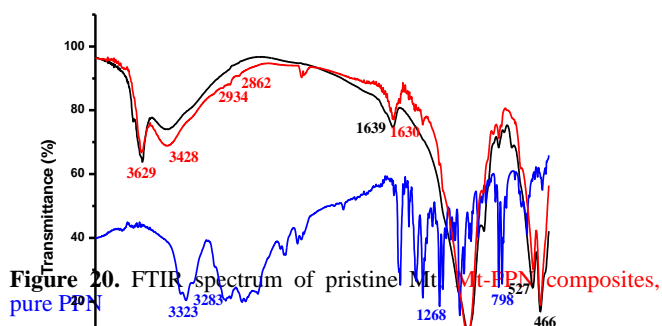


**Figure 20.** FTIR spectrum of pristine Mt, pure PPN, Mt-PPN composites.

The principal peaks depicted in the IR spectra of PPN occur at wavenumbers 1103, 1270, 772, 1580, 795 and 1240  $\text{cm}^{-1}$ . These peaks represent the stretching vibrations of the different functional groups that are present in the PPN structure. The wavenumbers 772 and 795 can be associated with the aromatic functional groups, 1240 and 1270 with the

amine functional group, 1103 with the OH group and 1580 with the ketone group respectively.<sup>43</sup>

The FT-IR spectrum of Mt has already been discussed under the section characterization of organoclay PF68-Mt.

In case of pristine Mt-PPN composites, peaks at 2934 and 2862 appear because of the C-H stretching of the  $\text{CH}_3$  group of PPN in the Mt-PPN composites. Not all characteristic bands belonging to Mt and PPN appear in the spectrum of PPN-Mt composites; several new bands in the region of 1250  $\text{cm}^{-1}$  to 1500  $\text{cm}^{-1}$  are also recognized. This also indicated that PPN interacts with the Mt layers.

However in the FT-IR spectra of organoclay PF68-Mt and PF68-Mt-PPN composites there is no significant difference was observed (Figure 21). The characteristic peaks related to PPN were not observed strengthening the fact of intercalation of PPN molecule with the organoclay PF68-Mt interlayer region.

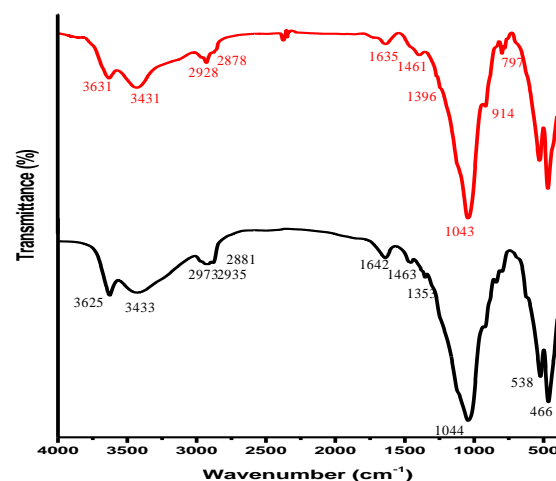


**Figure 21.** FTIR spectra: organoclay PF68-Mt, PF68-Mt-PPN composites

#### Zeta potential analysis

The zeta potential values of pristine Mt, organoclay PF68-Mt, pristine Mt-PPN composites and organoclay PF68-Mt-PPN composites at their natural pH in aqueous media were found to be negatively charged (Table 1). The negative charge of pristine Mt decreased after adsorption/intercalation of cationic drug PPN. Whereas, the same was increased after intercalation/surface adsorption of nonionic surfactant PF68, attributed to negatively charge terminal hydroxyl groups of poly oxy ethylene groups in PF68. When, organoclay PF68-Mt was used as an adsorbent for the PPN, it maintains the negative surface charge strengthening the fact of PPN intercalation within organoclay PF68-Mt layers as confirmed by XRD and FT-IR analysis.

**Table 1.** Zeta potential analysis

Code	Zeta potential (mV)
Pristine Mt	-33.9
Mt-PPN composites	-31.7
Organoclay PF68-Mt	-35.5



PF68-Mt-PPN composites	-35.3
------------------------	-------

### TG Studies

The TG thermogram of pristine Mt shows high thermal stability in the temperature region of 30-700 °C with weight loss of 10% from 30-150°C corresponds to the evaporation of free water and water bound to the cations present within the interlayer (Figure 22). Weight loss in the temperature range from 600-750 °C is due to the loss of hydroxyl groups in the aluminosilicate structure and at this point the structure of the Mt layers collapses.<sup>12,38,39</sup>

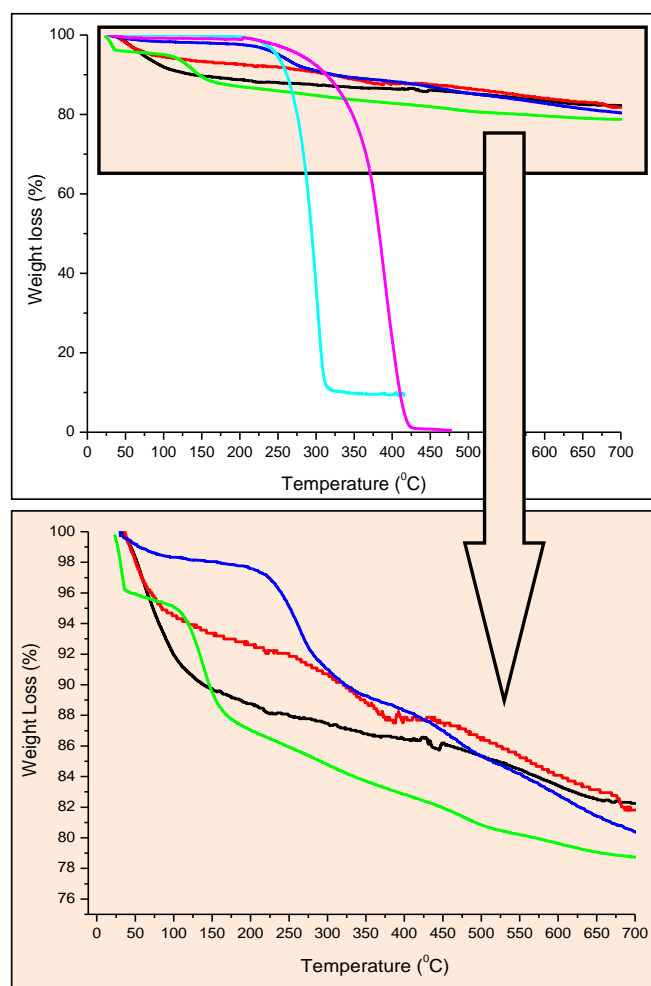


**Figure 22.** TG pattern: pristine Mt, PPN- Mt composites, organoclay PF68 - Mt, PF68-PPN- Mt composites, Pure PPN, Pure PF68

The thermogravimetric profile of pristine drug PPN (Figure 22) show a sharp weight loss at around 230-320°C corresponding to decomposition of the PPN molecule.<sup>44</sup> Pristine PF68 shows 100 % weight loss in the temperature range of 200 to 425°C.<sup>45</sup>

The pristine Mt-PPN composites (Figure 22) shows weight loss in three steps in the temperature region of 80-120 °C, 200-350 °C and 600-750 °C. The first weight loss of 6 % was observed from 80-150 °C suggesting replacement of interlayer water with PPN molecule. The weight loss observed was smaller than the pristine Mt (~10 %) because of the replacement of interlayer water with intercalated PPN which supposed to be stable and does not show any weight loss upto 200 °C. Weight loss from 600-750 °C might be attributed

to the loss of structural OH group in Mt-PPN composites. Decomposition of intercalated PPN within Mt layers took place in the temperature region of 250-400 °C evident by weight loss of 6 %.

In case of organoclay PF68-Mt, higher weight loss than PPN-Mt composites and degradation of PF68 at lower temperature than pure PF68 (Figure 21) was observed. Presence of less content of Mt is clearly evident from the thermo gram of organoclay PF68-Mt. When organoclay PF68-Mt was used for the adsorption of PPN, it shows the higher weight loss than PPN-Mt composites but less than PF68-Mt organoclay suggesting the fact of less surfactant content present within the PF68-PPN-Mt composites as has been concluded by XRD studies. Beside this, PF68-Mt-PPN composites follow the degradation pattern for both PF68 and PPN in the temperature range of 200-400 °C.

In case of pure Mt, pristine Mt-PPN composites, organoclay PF68 -Mt and PF68-Mt-PPN composites 82 %, 82 %, 80 % and 78 % residue was obtained in the temperature range of 20-700 °C, respectively, or otherwise it could be said that 18 %, 18 %, 20 % and 22 % weight loss was observed respectively. In case of PPN-Mt composites, replacement with PPN reduces the intercalated water content within Mt layers. Improved thermal stability of intercalated drug was also observed than the pure drug, followed by the same thermal behaviour as of pristine Mt.

### Scanning Electron Micrographic studies

The surface morphology of pristine Mt particles (Figure 23a) was in platelet form and displayed many flakes on the surface. The pristine Mt-PPN composites had irregular shapes as shown in Figure 23b.

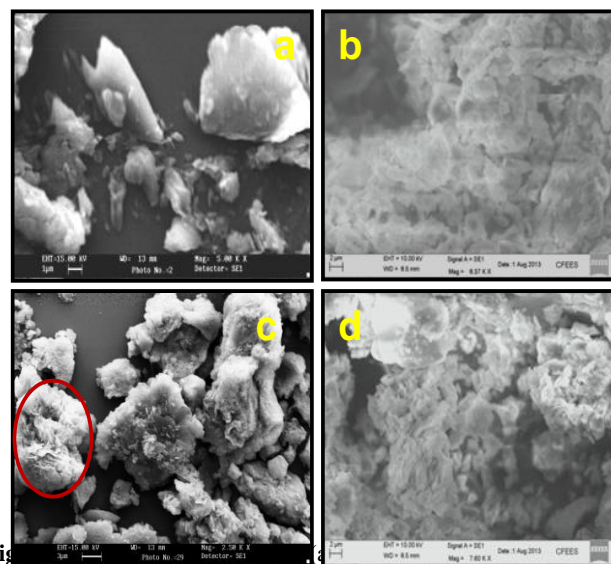


**Fig.** PPN composites (c) and PF68-Mt-PPN composites (d)

It has been found that the Mt-PPN composites had a different surface morphology when compared with that of pristine Mt alone as found to be more porous on surface leading to more open structure (encircled by red). Surface morphology of PF68-Mt-PPN composites were found to be irregular shaped particles with particle size in the range of 1-2 microns (Figure 22c). However no significant change in

the surface morphology as compared to organoclay PF68-Mt (Figure 22d) was observed.

#### Transmission electron micrographic studies

TEM images of pristine Mt clearly reveal the layered platelet structure of Mt with particle size in the range of 1.5 to 2  $\mu\text{m}$  (Figure 24a and b). TEM images of Mt-PPN composites are shown by (Figure 24 c and d). As a result of sonication required for sample preparation for TEM analysis, secretion of intercalated spherical drug particles of size 50-100 nm from Mt layers can be seen clearly (Figure 24c) further confirmed by the presence of PPN peak in UV spectra of sonicated sample of pristine Mt-PPN composites (Figure 24e).

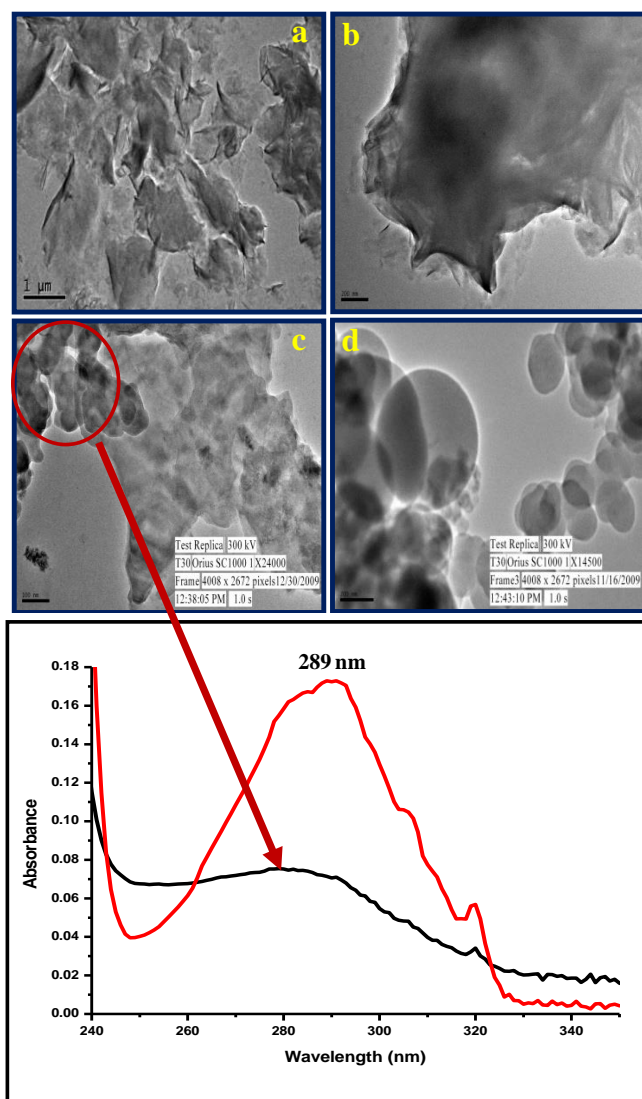


**Figure 24.** TEM images of pristine Mt (a and b) and Mt-PPN composites (c and d), UV spectra of aqueous PPN solution and sonicated Mt-PPN composites e.

#### In vitro drug release studies

In vitro release of pure PPN in simulated gastric (HCl, pH 1.2) and intestinal fluid (PBS, pH 7.4) at 37  $^{\circ}\text{C}$  was observed to be 84 % and 87 % (Figure 24) over a period of 4 h, respectively, approaches to 87 % and 90 % by the end of

8 h. In both the cases release pattern was not in a controlled manner (~ 36 % release per minute).<sup>12</sup>

When the pristine Mt-PPN composites exposed to the dissolution medium, the simultaneous penetration of the surrounding medium and cation exchange process occurred leading to a burst drug release of 40 % in simulated gastric fluid (SGF), and 23 % in simulated intestinal fluid (SIF) in initial first hour corresponds to adsorbed drug on the surface of the particles. Then the cation diffuses deep into the particles to exchange the drug, which leads to slow release of 57 % and 39 % by the end of 4 hours approaches to 75 % and 46 % by the end of 8 hours in SGF and SIF respectively (Figure 25). This study showed that release of PPN from the composites is controlled by a particle matrix that acts as diffusion barrier for drug release.<sup>25</sup> The difference in pH, presence of cations and higher solubility of PPN may be responsible for higher release of drug in acidic media. The percentage released of PPN was not up to 100 % probably due to the characteristic of ion-exchange reaction, i.e. this is an equilibrium process, and the interlayer cations cannot be exchanged completely.<sup>46,47</sup>

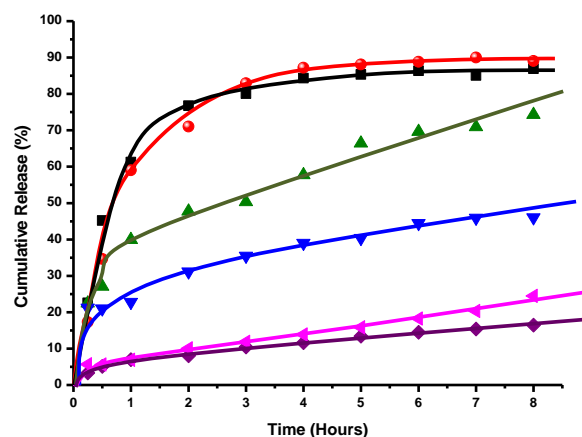


**Figure 25.** In vitro drug release profile in SGF (pH 1.2): pure PPN, Mt-PPN complex, PF68-Mt-PPN composites. In SIF (pH 7.4): pure PPN, Mt-PPN complex, PF68-Mt-PPN composites

In case of PF68-Mt-PPN composites, initial burst release was substantially controlled by the presence of PF68 in both the dissolution media as only 7 % drug release was observed within first hour which approaches to 13 % and 11 % by the end of 4 h. The cumulative drug release of 16.4 % and 24.5 % over a period of 8 hours in SGF and SIF was obtained respectively which approaches to 20.9 % and 38.96 % by the end of 24 h (data not shown). In the present case it has been proposed that, triblock copolymer PF68 was intercalated within Mt layers in the form of micelles. So, the diffusion process is suggested to be responsible for the drug release from organoclay PF68-Mt. As a result of the interaction of PPN with hydrophilic parts of PF68 (PF 68 corona) the hydrophilic-hydrophilic interaction may prevents the release of drug in the dissolution media. However less release in SGF (HCl pH 1.2) is might be corresponds to the stability of Mt layers within the acidic media. Whereas, in case of pristine Mt, simply ion exchange process was the main driving force for release of drug in the dissolution media resulting in comparatively faster drug release process.

In vitro drug release data suggest that organoclay PF68-Mt-PPN composites are able to retain the high amount of PPN in simulated gastric fluid (the desired site of absorption), as compared to pristine Mt-PPN composites, with the advantage of gradual drug release over a longer period of time, thus able to increase the absorption, improve drug efficacy, and decrease dose requirements.

## CONCLUSION

In the present work Pluronic F68 a non-ionic triblock copolymer has been reported for the first time for synthesis of organoclay PF68-Mt organoclay. The intercalation of PF68 moiety was confirmed by XRD, FT-IR, zeta potential and thermal studies.

The feasibility study of developed PF68-Mt organoclay is further being explored as a drug delivery vehicle for propranolol HCl, an antihypertension drug.

The developed PF68-Mt-PPN composites were compared for their physiochemical properties and in vitro drug release behaviour with pristine Mt-PPN composites.

In case of pristine Mt-PPN composites developed by ion exchange/adsorption method, 127 mg g<sup>-1</sup> of PPN was found to adsorb on the Mt surface. Intercalation of PPN was confirmed by XRD, FTIR, zeta potential and thermal studies. In vitro drug release profile of pristine Mt-PPN composites shows PPN release in simulated intestinal fluid was more sustained as compared to simulated gastric fluid over a period of 8 h governs by ion exchange process.

Organoclay PF68-Mt reveals enhanced negative surface charge with high adsorption capacity as compared to pristine Mt as adsorption capacity increase upto 171 mg g<sup>-1</sup>. XRD studies suggested that organoclay PF68-Mt possesses highest d spacing followed by PF68-Mt-PPN composites, Mt-PPN composites and pristine Mt and confirms the intercalation of PPN within organoclay PF68 layers.

In vitro drug release profile of PF68-Mt-PPN composites suggest that, presence of intercalated PF68 in the composites significantly retarded the release of PPN in simulated gastric and intestinal fluid as compared to pristine Mt. The sustained release pattern of PPN might be attributed to the interaction of PPN with hydrophilic parts of PF68 intercalated within Mt layers.

Thus the developed PF68-Mt-PPN composites have promising potential to sustain the release of PPN than pristine Mt, able to reduce the dosing frequency and associated side effects. The obtained preliminary results suggest that synergism of FDA approved biocompatible Mt and Pluronic F68 can be further explored as a successful formulation of PPN as oral and sustained release drug delivery vehicle.

## ACKNOWLEDGMENT

Authors express their sincere thanks to the Head, Department of Chemistry, Director, USIC, University of

Delhi for providing instrumentation facilities. Ms. Seema is thankful to UGC/RGNF for providing financial assistance for this research work under the project of sch/rgnf/srf/f-10/2007-08.

## REFERENCES

- <sup>1</sup>Borkar, S. R., Sawant, S. N., Shende, V. A., Dimple, S. K., *Int. J. Pharm. Sci. Nanotech.*, **2010**, *3*, 901–905.
- <sup>2</sup>Rodrigues, L. A. S., Figueiras, A., Veiga, F., de Freitas, R. M., Nunes, L. C. C., da Silva Filho, E. C., da Silva Leite, C. M., *Coll. Surf. B: Biointerfaces*, **2013**, *103*, 642–651.
- <sup>3</sup>de Paiva, L. B., Morales, A. R., Valenzuela Diaz, F. R., *Appl. Clay Sci.*, **2008**, *42*, 8–24.
- <sup>4</sup>Gournis, D., Jankovicic, L., Maccallini, E., Benne, D., Rudolf, P., Colomer, J., Sooambar, C., Georgakilas, V., Prato, M., Fanti, M., Zerbetto, F., Sarova, G. H., Guldi, D. M. *J. Am. Chem. Soc.* **2006**, *128*, 6154–6163.
- <sup>5</sup>Gournis, D., Georgakilas, V., Karakassides, M. A., Bakas, T., Kordatos, K., Prato, M., Fanti, M., Zerbetto, F., *J. Am. Chem. Soc.*, **2004**, *126*, 8561–8568.
- <sup>6</sup>Guegan, R., Gautier, M., Beny, J. M., Muller, F., *Clays Clay Miner.*, **2009**, *57*, 502–509.
- <sup>7</sup>Gautier, M., Muller, F., Leforestier, L., Beny, J. M., Guegan, R. *Appl. Clay Sci.*, **2010**, *49*(3), 247–254.
- <sup>8</sup>Chua, Y. C., Lu, X., *Langmuir*, **2007**, *23*, 1701–1710.
- <sup>9</sup>Othmani-Assmann, H., Benna-Zayani, M., Geiger, S., Fraisse, B., Kbir-Arighib, N., Trabelsi Ayadi, M., Ghermani, N. E., Grossiord, J. L., *J. Phys. Chem., C*, **2007**, *111*, 10869–10877.
- <sup>10</sup>Lee, S. Y., Cho, W. J., Hahn, P. S., Lee, M., Lee, Y. B., Kim, K. J., *Appl. Clay Sci.*, **2005**, *30*, 174–180.
- <sup>11</sup>Dong Y., Feng S. S. *Biomaterials*, **2005**, *26*, 6068–6076.
- <sup>12</sup>Seema, Datta M., *Appl. Clay Sci.*, **2013**, *80–81*, 85–92.
- <sup>13</sup>Seema, Datta M., *Int. J. Pharm. Pharm. Sci.*, **2013**, *5*(2), 332–341.
- <sup>14</sup>Seema, Datta M., *Eur. Chem. Bull.*, **2013**, *2*(11), 942–951.
- <sup>15</sup>Kaur M., Datta M., *Adsorpt. Sci. Technol.*, **2011**, *29*(3), 309–318.
- <sup>16</sup>Gelfer, M., Burger, C., Fadeev, A., Sics, I., Chu, B., Hsiao, B. S., Heintz, A., Kojo, K., Hsu, S., Si, M., Rafailovich, M., *Langmuir* **2004**, *20*, 3746–3758.
- <sup>17</sup>Guegan, R., *Langmuir*, **2010**, *26*(24), 19175–19180.
- <sup>18</sup>Guegan, R., Gautier, M., Beny, J. M., Muller, F., *Clays Clay Miner.*, **2009**, *57*(4), 502–509, 2009.
- <sup>19</sup>Batrakova, E. V., Kabanov, A. V., *J. Controll. Release*, **2008**, *130*, 98–106.
- <sup>20</sup>Batrakova, E. V., Alakhov V. Yu., *J. Controll. Release*, **2002**, *82*, 189–212.
- <sup>21</sup>Alexandridis, P., Hatton, T. A., *Colloids Surfaces A: Physicochem. Eng. Aspects*, **1995**, *96*, 1–46.
- <sup>22</sup>Schmolka, I. R., *J. Am. Oil Chem. Soc.*, **1977**, *54*, 110–116.
- <sup>23</sup>Dollery, S. C., *Therapeutic Drugs*. Churchill Livingstone, Edinburgh **1991**. 272–278.
- <sup>24</sup>Chaturvedi, K., Umadevi, S., Vaghani, S., *Sci. Pharm.*, **2010**, *78*, 927–939.
- <sup>25</sup>Rojtanatanya, S., Pongjanyakul, T., *Int. J. Pharm.*, **2010**, *383*(1–2), 106–115.
- <sup>26</sup>Patra, C.N., Kumar, A. B., Pandit, H. K., Singh, S. K., Devi, M. V., *Acta Pharm.*, **2007**, *57*, 479–489.
- <sup>27</sup>Paker-Leggs, S., Neau, S. H., *Int. J. Pharm.*, **2009**, *369*, 96–104.

- <sup>28</sup>Nagarwal R. C., Singh P. N., Shri Kant, Maiti P., Pandit J. K. *Chem. Pharm. Bull.*, **2011**, *59* (2), 272-278.
- <sup>29</sup>Joshi, G. V., Kevadiya, B. D., Patel, H. A., Bajaj, H. C., Jasra R.V., *Int. J. Pharm.*, **2009**, *374*, 53-57.
- <sup>30</sup>Joshi, G.V., Kevadiya, B.D., Bajaj, H.C., *Micropor. Mesopor. Mater.*, **2010**, *132*, 526-530.
- <sup>31</sup>Park, J. K., Choy, Y. B. Oh, J. M., Kim, J. Y., Hwang, S. J., Choy, J. H., *Int. J. Pharm.*, **2008**, *359*, 198-204.
- <sup>32</sup>Joshi, G. V., Patel, H. A., Kevadiya, B. D., Bajaj, H. C., *Appl. Clay Sci.* **2009**, *45*, 248-253.
- <sup>33</sup>Chen B.Y., Lee Y. H., Lin W. C., Lin F. H., Lin K. F., *Biomed. Eng. Appl. Basis Commun.*, **2006**, *18*(1), 30-36.
- <sup>34</sup>Meng, N., Zhou, N. L., Zhang, S. Q., Shen, J., *Int. J. Pharm.*, **2009**, *382*, 45-49.
- <sup>35</sup>Sahu, A., Kasoju, N., Goswami P., Utpal Bora, *J. Biomater. Appl.* DOI: 10.1177/0885328209357110.
- <sup>36</sup>Guegan, R, *Langmuir* **2010**, *26*(24), 19175-19180.
- <sup>37</sup>Zhao, D., Huo, Q., Feng, J., Chmelka, B. F., Stucky, G. D., *J. Am. Chem. Soc.*, **1998**, *120* (24), 6024-6036.
- <sup>39</sup>Chen, Y., Zhou, A., Liu, B., Liang, J., *Appl. Clay Sci.* **2010**, *49*(3), 108-112.
- <sup>40</sup>Passerini, N., Albertini, B., Gonzalez-Rodriguez M. L., Cavallari, C., Rodriguez, L., *Eur. J. Pharm. Sci.* **2002**, *15*, 71-78
- <sup>41</sup>[http:// Propranolol Information from Drugs.com.htm](http://Propranolol Information from Drugs.com.htm).
- <sup>42</sup>Patra, C. N., Kumar, A. B., Pandit, H. K., Singh, S. K., Devi, M. V., *Acta Pharm.*, **2007**, *57*, 479-489.
- <sup>43</sup>Sharan, G., Dey, B. K., Nagarajan, K., Das, S., Kumar, S. V., Dinesh, V., *Int. J. Pharm. Pharm. Sci.*, **2010**, *2*(2), 21-31.
- <sup>44</sup>Macedo, R. O., Nascimento T. Gomes Do., Veras, J. W. E., *J. Therm. Anal. Calor.*, **2002**, *67*, 483-489.
- <sup>45</sup>Wang, T., Wu, Y., Zeng, A. J., *Appl. Polym. Sci.*, **2009**, 605-613.
- <sup>46</sup>Joshi, G. V., Kevadiya, B. D., Patel, H. A., Bajaj, H. C., Jasra, R. V., *Int. J. Pharm.*, **2009**, 53-57.
- <sup>47</sup>Nunes, C. D., Vaz, P. D., Fernandes, A. C., Ferreira, P., Roma, C. C., Calhorda, M. J. *Eur. J. Pharm. Biopharm.*, **2007**, *66*, 357-365.

Received: 31.03.2014

Accepted: 30.04.2014.

<sup>38</sup>Lakshmi, M. S., Sriranjani, M., Bakrudeen, H. B., Kannan, A. S., Mandal, A. B., Reddy, B. S.R., *Appl. Clay Sci.*, **2010**, *48*, 589-592.